

Magic Messengers in Gauge Mediation and signal for 125 GeV boosted Higgs boson

Pritibhajan Byakti*

Theory Division, Saha Institute of Nuclear Physics, 1/AF Bidhan Nagar, Kolkata-700064, India.

Diptimoy Ghosh†

Tata Institute of Fundamental Research, Homi Bhabha Road, Mumbai-400005, India.

We consider a renormalizable messenger sector with magic messenger fields instead of usual SU(5) complete multiplets. We derive the soft supersymmetry breaking terms and show that the gaugino sector can be parameterized by only two parameters. These parameters can be chosen appropriately to obtain various patterns of gaugino masses and different ratios among them. The sfermion sector can also be characterized by two independent parameters which can be adjusted to change the relative masses of squarks and sleptons. A judicious choice of parameters also allows us to achieve the lightest Higgs boson mass about 125 GeV. In this paper we focus on a scenario where a comparatively large hierarchy exists between the U(1) and SU(2) gaugino mass parameters. In such a case, the lightest Higgs boson originating from the decay of the next-to-lightest neutralino, following the direct production of chargino neutralino pair, can be considerably boosted. We show that a boosted Supersymmetric Higgs signal with a decent signal to background ratio can be obtained using the jet substructure technique at LHC with 8 TeV (14 TeV) center of mass energy and an integrated luminosity of about 30 fb⁻¹ (15 fb⁻¹).

arXiv:1204.0415v2 [hep-ph] 9 Nov 2012

* pritibhajan.byakti@saha.ac.in

† diptimoyghosh@theory.tifr.res.in

I. INTRODUCTION

The performance of the Large Hadron Collider (LHC) at CERN has been extraordinary in the last year and data of about 5 fb^{-1} has been already collected by each of the two major experimental groups CMS and ATLAS. With the data already accumulated, the LHC has left the LEP and Tevatron results far behind in many of the search channels. But, apart from the recent hint [1, 2] about a possible 124 – 126 GeV Higgs boson, no other signal of any new physics (NP) has been reported yet.

The Minimally Supersymmetric Standard Model (MSSM) which is undoubtedly one of the most studied models beyond the Standard Model (SM) has been a benchmark for the LHC searches and limits on Supersymmetric particles have been shown by both the ATLAS and CMS collaborations [3].

Supersymmetry (SUSY) [4, 5] which is a beautiful theoretical idea by its own right has been in the spotlight among the phenomenologists for a long time because of its ability to tame the quadratic divergence in the scalar sector of the SM elegantly. However if SUSY has to be realized in nature, it must be broken so that it does not contradict experimental observations. From a theoretical point of view, one would expect that the SUSY is broken spontaneously so that the underlying microscopic Lagrangian is SUSY invariant but the vacuum state is not. This is the same mechanism which keeps the electroweak symmetry hidden at low energies. There is no consensus about how SUSY must be broken at high energies but by whichever way it is broken, at the electroweak scale the effect of SUSY breaking can always be parameterized by introducing additional terms in the Lagrangian which break SUSY explicitly. But these terms should only include operators which do not bring back the quadratic divergences from the quantum corrections to the scalar masses. These are called the SUSY breaking soft terms, all of which have positive mass dimension.

Unfortunately, spontaneous breaking of SUSY in a phenomenologically acceptable way has not been achieved till now with only tree level renormalizable interactions. This problem has been solved by breaking SUSY in a sector, the so called “hidden sector”, which has either no coupling or very small direct coupling to the MSSM fields. However, there are some mediating interactions which carry the information of SUSY breaking from the hidden sector to the MSSM and generate the soft terms. The gravitational interaction as a mediator of SUSY breaking has been the most popular scenario historically [6]. Another very popular mechanism has been the so called “Gauge Mediated SUSY Breaking (GMSB)” [7–12] scenario where the soft terms are generated through loops involving some messenger fields. These messenger fields couples to the SUSY breaking sector and also have SM gauge group quantum numbers. As gauge interactions are flavor diagonal, this mechanism also has the advantage of automatically being flavor-blind which is phenomenologically attractive from the points of view of Flavor Changing Neutral Currents (FCNC).

The General gauge mediation (GGM), a framework developed by Meade, Seiberg, and Shih [13] generalizes models of gauge mediation to accommodate arbitrary hidden sectors including those which are not necessarily weakly coupled. It was shown in GGM that the soft masses of MSSM gauginos and sfermions, to leading order in the SM gauge interactions, can be expressed in terms of the hidden sector current correlation functions. Extension of this framework has been studied in [14–20]. It was also shown in a model independent way that non-universal gaugino masses can be obtained in GGM without spoiling the gauge-coupling unification. By universality in gaugino masses we mean that these masses at any scale are proportional to the corresponding gauge couplings at that scale. However, in weakly coupled GMSB scenarios with complete multiplets of SU(5) messengers the gaugino masses remain universal. In general messenger models [21, 22], one can achieve non-universal gaugino masses but the masses of the messenger fields get constrained in order to maintain gauge coupling unification.

It was shown in [23] that one can achieve unification of gauge couplings even if the new fields added at some intermediate scales do not form complete multiplets of SU(5) and the unification is independent of the scale at which these fields are added. These specially chosen fields were termed as “Magic” fields and they were used in ordinary gauge mediation in order to get non universal gaugino masses with extremely large hierarchy, 1:30:200 among the U(1), SU(2) and SU(3) gaugino mass parameters [23], which is phenomenologically not interesting. Also the obtained patterns of mass ratios were not very flexible.

In this paper we generalize their idea and write the superpotential containing all possible renormalizable terms for the messenger sector. We derive the soft SUSY breaking terms and show that the gaugino sector can be described by two independent parameters which can be tuned to achieve almost any ratio of gaugino masses. This is a novel feature of our models. We also show that the sfermion sector in this class of models can also be parameterized by two parameters which can be chosen to adjust the relative masses of squarks and sfermions. In this class of models the squark masses can be equal to the Higgs mass parameters m_{H_u} and m_{H_d} at the messenger scale which can lead to a small value of the Higgsino mass parameter μ and thus, a Higgsino-like NLSP (like models of extra ordinary gauge mediation (EOGM) with doublet triplet splitting [24]). Some region of the parameter space of this model also allows for the lightest SUSY Higgs mass about 125 GeV.

We consider a phenomenologically interesting scenario where the ratio of the U(1) and SU(2) gaugino mass parameters at the electroweak scale is comparatively larger than the universal case 1:2. In this case, because of the

comparatively larger splitting between the next-to-lightest neutralino lightest (χ_2^0) and the neutralino (χ_1^0), the Higgs boson (h) coming from the decay $\chi_2^0 \rightarrow \chi_1^0 h$ is quite boosted. Motivated by this, we study the $\ell + b\bar{b} + \cancel{p}_T$ channel to look for SUSY Higgs boson using the jet substructure technique.

The paper is organized as follows. In the next section we briefly review the concept of magic fields. In Sec.III, we describe our models and then study the mass spectrum of gauginos and sfermions. The phenomenology of an explicit model of this class of models is discussed in Sec. IV A. We close our discussion in Sec. V with a brief summary of our findings.

II. MAGIC FIELDS AND UNIFICATION

In this section we will review the concept of magic fields and derive some relations which will be useful later in this paper. It is well known that, if no additional matter field is added in the intermediate scale, the SM gauge couplings get unified in the MSSM at the scale $M_0 \sim 2.0 \times 10^{16}$ GeV. In general, assuming that the gauge couplings unify at some scale M_{GUT} , their one loop Renormalization Group (RG) equations reads,

$$\alpha_a^{-1}(\mu) = -\frac{b^a}{2\pi} \ln \frac{\mu}{M_{GUT}} + \alpha^{-1}(M_{GUT}), \quad (1)$$

where the index $a = 1, 2, 3$ represent the SM gauge groups $U(1)$, $SU(2)$ and $SU(3)$ respectively and b_a are the corresponding beta functions. In the MSSM we have $b^a = b_0^a = \{\frac{33}{5}, 1, -3\}$.

At any value of μ , Eq. (1) is an equation of a straight line in α^{-1} and b . It directly follows that for the unification of the gauge couplings, α_a^{-1} and b_a must respect the following relation,

$$\frac{\alpha_3^{-1} - \alpha_2^{-1}}{\alpha_2^{-1} - \alpha_1^{-1}} = \frac{b^3 - b^2}{b^2 - b^1}. \quad (2)$$

Even if matter fields are added at some intermediate scale, the gauge coupling unification can be maintained (at one loop) so far as Eq. (2) is satisfied. The fields whose beta functions are such that they do not spoil Eq. (2) are called Magic fields.

Using the one-loop RG equation of Eq. (1) in the MSSM one has,

$$\alpha_a^{-1}(M_Z) - \alpha_b^{-1}(M_Z) = -\frac{b_0^a - b_0^b}{2\pi} \log \frac{M_Z}{M_0}. \quad (3)$$

We now add matter fields at some intermediate scales and assume that fields added at the scale m_i contribute to the beta functions by an amount d_i^a (dynkin index of that field). The gauge couplings at any scale μ can now be written as,

$$\alpha_a^{-1}(\mu) = \alpha_a^{-1}(M_Z) - \frac{b_0^a}{2\pi} \log \frac{\mu}{M_Z} - \sum_{i \text{ with } m_i < \mu} \frac{d_i^a}{2\pi} \log \frac{\mu}{m_i}. \quad (4)$$

If we now choose

$$d_i^a - d_i^b = k_i (b_0^a - b_0^b), \quad (5)$$

then it is clear that Eq. (2) will remain intact. Hence we can achieve gauge coupling unification even with the presence of intermediate mass scales and this is independent of the values of m_i . But unlike complete multiplets of say, $SU(5)$ the unification scale changes in this case [25]. Let us assume that the gauge coupling constants now unify at a scale M_{GUT} . We can now rewrite Eq. (3) as,

$$\alpha_a^{-1}(M_Z) - \alpha_b^{-1}(M_Z) = -\frac{b_0^a - b_0^b}{2\pi} \log \frac{M_Z}{M_{GUT}} - \sum_{i=1, \dots, N} \frac{d_i^a - d_i^b}{2\pi} \log \frac{m_i}{M_{GUT}}. \quad (6)$$

Comparing Eq. (3) and (6) we can now write the new unification scale M_{GUT} in terms of the unification scale M_0 in the MSSM,

$$M_{GUT} = M_0 \prod_{i=1, 2, \dots, N} \left(\frac{m_i}{M_0} \right)^{\kappa_i}, \text{ where } \kappa_i = k_i / \left(1 + \sum_{j=1, 2, \dots, N} k_j \right). \quad (7)$$

The change in the unified value of the gauge couplings, $\delta\alpha^{-1}(M_{GUT})$ can also be written down explicitly,

$$\delta\alpha^{-1}(M_{GUT}) = \frac{1}{2\pi} \sum_{i=1,2,\dots,N} \left(d_i^a - \kappa_i b_0^a - \kappa_i \sum_{j=1,2,\dots,N} d_j^a \right) \log \frac{m_i}{M_0}. \quad (8)$$

An example of magic fields is the combination of fields $\phi_Q, \phi_{\overline{Q}}$ and ϕ_G whose transformation properties under the SM gauge group are given by $(3, 2)_{\frac{1}{6}}, (\overline{3}, 2)_{-\frac{1}{6}}$ and $(8, 1)_0$ respectively. Here the first number in the bracket is the SU(3) representation and the second number refers to the SU(2) representation. The number outside the bracket is the Hypercharge of the multiplet. Note that the individual fields above are not magic fields but the combination as a whole satisfies the magic field condition of Eq. (5). The set of fields mentioned above can be obtained from the SO(10) complete multiplets $16, \overline{16}$ and 45 after spontaneous symmetry breaking [23].

III. MASS SPECTRUM OF THE MAGIC MESSENGER MODELS

In this section, we will derive some general properties of the magic messenger models where, unlike models of ordinary gauge mediation, the superpotential also contains bare mass terms allowed by symmetry. But before we go to the details of our model, let us first discuss those models of GMSB where non-universal gaugino masses have been obtained and their qualitative differences with our model.

In ordinary gauge mediation models the messenger fields are complete multiples of SU(5) like $5 \oplus \overline{5}$. Addition of such complete multiplets changes the beta functions equally for all the SM gauge groups at any scale. Clearly this does not change the universality of the gaugino masses. Even if all possible renormalizable terms are considered in the superpotential, the situation does not change and universality is maintained. But instead of SU(5) multiplets if one uses SU(2) and SU(3) irreducible representations and write the most general superpotential (like models of EOGM with doublet triplet splitting [24]), then non-universal gaugino masses can be achieved only if these doublets and triplets are charged differently under some global symmetry. But to achieve gauge coupling unification at the same time the masses of the messenger fields should satisfy some constraints. In generalized messenger models, one can easily obtain non-universal gaugino masses but this type of models generally bypass the question of unification by arguing that there may be some other fields (not messenger of SUSY breaking) in the theory which are charged under the SM and using these fields it is always possible to get successful unification. If one does not assume this then messenger masses get constrained again. Another generalized messenger model is also available in the literature [26] where messenger masses are not constrained but the GUT used there is an anomalous U(1) GUT.

The models we are proposing are also generalized messenger models but here the messenger fields are magic fields. This class of models has two main differences with other generalized messenger models: (a) gauge coupling unification is independent of messenger scales and (b) changes in beta functions for each added messenger satisfy the magic relation of Eq. (5). The second property has non-trivial consequences as we will see in the next two sections.

A. The models

Our models consists of (1) N pairs of magic messenger fields, each pair consisting of $(\phi, \tilde{\phi})$ where ϕ ($\tilde{\phi}$) transforms under some representation (its conjugate representation) of the SM gauge group, and (2) a spurion field X which is a standard model gauge singlet but can have charges under some other symmetries like the R-symmetry. Note that these ϕ fields are in general not single irreducible representations; they can be a set of fields (each transforming under an irreducible representation) which satisfy the magic condition of Eq. (5). We assume that the field X gets a vacuum expectation value (VEV) through some dynamics of the hidden sector: $\langle X \rangle = M + \theta^2 F$. For the sake of calculational simplicity we make the assumption that two different pairs of magic messengers either transform under the same representation of the gauge group or have no constituent fields having the same transformation property. This allows us to sub-divide the messenger field pairs into different sets (labeled by p) where all members of a set have the same representation. Note that a set may consist of either one pair of messenger fields or many pairs of them. We label the different members (a particular pair of magic messengers) of a set p by the index i_p . For example, if a particular set p has five pairs of magic messengers then i_p runs from 1 to 5. We now write the renormalizable superpotential to be,

$$W = \sum_p \sum_{i_p, j_p} \left(\lambda_{i_p j_p}^p X + m_{i_p j_p}^p \right) \tilde{\phi}_{i_p} \phi_{j_p}, \quad (9)$$

where the form of the matrices λ^p and m^p are determined by global (R and/or non-R) symmetries of the theory. Note that, in general different constituent fields of any magic field can get different masses and couplings. But to

form a magic field, these constituent fields need to share the same mass. We treat the magic fields (ϕ_{i_p} 's) 'as if they are irreducible representations of some group' and write the couplings in the superpotential because this assumption automatically ensures the above requirement (of equality of the masses of the constituent fields of each the magic messenger fields). The above superpotential is symmetric under the interchange of ϕ_{i_p} field with $\tilde{\phi}_{i_p}$ and vice versa. This symmetry is called the messenger parity and it helps us to get rid of the dangerous Fayet-Iliopoulos (FI) terms.¹ Throughout this paper we will call this class of models as "Magic Messengers in Gauge Mediation (MMGM)".

To calculate the soft-terms, we need to write the Lagrangian in mass eigenstates of fermion fields and scalar fields. Using bi-unitary transformations on the superfields, we first make fermion mass matrices of each set diagonal and real: $M_f^p = \text{diag}(\dots, m_{i_p}, \dots)$. In this basis the Kähler term will not change. The matrices $\lambda^p F$ will change but for brevity we keep the same symbols. Messenger parity and CP conservation imply that these matrices should be real and symmetric. Going to the basis $\phi_{\pm p} = \frac{1}{\sqrt{2}}(\dots, \phi_{i_p} \pm \phi_{i_p}^*, \dots)^T$, we can bring sfermion mass squared matrix of any set in the block-diagonal form with two blocks: $M_{\pm p}^2 = (M_f^p)^2 \pm \lambda^p F$. Now these two matrices can be diagonalized as $U_{\pm}^{p\dagger} M_{\pm p}^2 U_{\pm}^p$ with eigenvalues $m_{\pm i_p}^2$. We define the following combinations of U matrices which will be used in the next section,

$$\mathcal{A}_{i_p j_p}^{p\pm} = U_{\pm i_p j_p}^{p\dagger} U_{\pm j_p i_p}^p \text{ and } \mathcal{B}_{i_p j_p} = \sum_{k_p l_p} (U_{+i_p k_p}^{p\dagger} U_{-k_p j_p}) (U_{-j_p l_p}^{p\dagger} U_{+l_p i_p}). \quad (10)$$

B. Gaugino masses

The expression for gaugino masses at the messenger scale can be written as,

$$M_a = \frac{\alpha_a}{4\pi} \sum_p d_p^a \Lambda_p^G \quad (11)$$

where d_p^a is the dynkin index of the magic messenger pairs in the set labeled by p corresponding to the gauge group label a , the superscript G in Λ refers to the gaugino sector, and Λ_p^G is given by [22]

$$\Lambda_p^G = 2 \sum_{i_p, j_p \pm} (\pm) \mathcal{A}_{j_p i_p}^{p\pm} \frac{m_{i_p} m_{\pm j_p}^2}{m_{\pm j_p}^2 - m_{i_p}^2} \log \left(\frac{m_{\pm j_p}}{m_{i_p}} \right)^2. \quad (12)$$

Here Λ_p^G are independent of the SM gauge group. However the presence of d_p^a in the expression for gaugino masses implies that the ratio of gaugino masses is not equal to the ratio of α_a 's. This means that the gaugino masses are non-universal in this class of models. Apparently it seems that the gaugino masses are completely independent, but actually this is not true. Their ratio satisfies some beautiful structure. The ratio of the gaugino masses can be written as,

$$M_1 : M_2 : M_3 = 1 : \frac{\alpha_2}{\alpha_1} \left[1 + (b_0^{(2)} - b_0^{(1)}) \zeta \right] : \frac{\alpha_3}{\alpha_1} \left[1 + (b_0^{(3)} - b_0^{(1)}) \zeta \right], \quad (13)$$

where

$$\zeta = \frac{\sum_p k_p \Lambda_p^G}{\sum_p d_p^{(1)} \Lambda_p^G}. \quad (14)$$

The value of ζ can be zero, positive or negative. All the gaugino mass parameters become equal if

$$\zeta = \zeta_0 = -\frac{\alpha_3 - \alpha_2}{\alpha_3(b_0^{(3)} - b_0^{(1)}) - \alpha_2(b_0^{(2)} - b_0^{(1)})} = -\frac{\alpha_2 - \alpha_1}{\alpha_2(b_0^{(2)} - b_0^{(1)})},$$

where in the last step we used Eq. (2). Any arbitrary ζ can always be written as

$$\zeta = \zeta_0 + \tilde{\zeta}. \quad (15)$$

¹ This FI term is proportional to the VEV of the scalar component of the U(1) current superfield J . Under messenger parity $J \rightarrow -J$, because the fields ϕ_{i_p} transform under the conjugate representation of the fields ϕ_{i_p} . Hence, due to messenger parity, VEV of J vanishes [13, 16].

In that case Eq. (13) takes the form,

$$\begin{aligned} M_1 : M_2 : M_3 &= 1 : 1 + \frac{\alpha_2}{\alpha_1} (b_0^{(2)} - b_0^{(1)}) \tilde{\zeta} : 1 + \frac{\alpha_3}{\alpha_1} (b_0^{(3)} - b_0^{(1)}) \tilde{\zeta}, \\ &= 1 : 1 - \frac{28}{5} \frac{\alpha_2}{\alpha_1} \tilde{\zeta} : 1 - \frac{48}{5} \frac{\alpha_3}{\alpha_1} \tilde{\zeta}. \end{aligned} \quad (16)$$

It is now clear from Eq. (16) that various ratios among the gaugino masses can be obtained, (a) for negative $\tilde{\zeta}$, one gets normal hierarchy, (b) for $\tilde{\zeta} = 0$, all the gaugino masses are equal, and, (c) for non-zero positive $\zeta \leq \frac{5\alpha_1}{48\alpha_3}$, one gets inverted hierarchy. For $\zeta > \frac{5\alpha_1}{48\alpha_3}$, some more patterns can be achieved.

So to conclude this section, the gaugino sector of this class of models can be parametrized by two free parameters: one of them can be taken as the mass of the U(1) gaugino and the other one is the ζ (or $\tilde{\zeta}$) parameter. These two parameters can be tuned to get phenomenologically interesting ratios among the gaugino masses.

C. Sfermion masses

The sfermion masses are obtained at the two loop level in GMSB. In GGM, these are parameterized by three parameters A_a ($a = 1, 2, 3$) for three gauge groups U(1), SU(2) and SU(3). In terms of these three parameters the expression for the sfermion masses [13] can be written as follows,

$$m_{\tilde{f}}^2 = \sum_a g^4 c_2(f, a) A_a, \quad (17)$$

where $c_2(f, a)$ is the quadratic Casimir of the representation f of the gauge group a . In our class of models the expression for A_a turns out to be

$$A_a = 2 \frac{1}{(16\pi^2)^2} \sum_p d_p^a \Lambda_p^S \quad (18)$$

where Λ_p^S is given by [22],

$$\begin{aligned} \Lambda_p^S &= 2 \sum_{i_p j_p \pm} m_{\pm i_p}^2 \left[\mathcal{A}_{i_p j_p}^{p\pm} \log \left(\frac{m_{\pm i_p}^2}{m_{j_p}^2} \right) - 2 \mathcal{A}_{i_p j_p}^{p\pm} Li_2 \left(1 - \frac{m_{j_p}^2}{m_{\pm i_p}^2} \right) \right. \\ &\quad \left. + \frac{1}{2} \mathcal{B}_{i_p j_p} Li_2 \left(1 - \frac{m_{\mp j_p}^2}{m_{\pm i_p}^2} \right) \right]. \end{aligned} \quad (19)$$

The quantities Λ_p^S and A_a are required to be strictly positive in order to have positive sfermion masses.

Ratio of the A_a parameters can be written as,

$$A_1 : A_2 : A_3 = 1 : 1 - \frac{28}{5} \eta : 1 - \frac{48}{5} \eta, \quad (20)$$

where

$$\eta = \frac{\sum_p k_p \Lambda_p^S}{\sum_p d_p^{(1)} \Lambda_p^S}. \quad (21)$$

Note that η cannot be greater than $\eta_0 = \frac{5}{48}$. For $\eta \sim \eta_0$, one has $A_1 > A_2 \gg A_3$. In this limit, from Eq. (17) one can see that soft SUSY breaking squark and Higgs masses will be approximately same (universal) at the messenger scale. This would in turn render the value of m_{H_u} at weak scale insensitive to the universal scalar masses in the ultraviolet. This can be understood as a consequence of a ‘‘focus point’’ in the RG behavior of m_{H_u} [27, 28]. In this case it is possible to have a small μ (supersymmetric mass term for the Higgs) [29, 30] and thus, a Higgsino like NLSP. This can lead to very distinct phenomenology [31, 32].

IV. AN EXPLICIT MODEL OF MMGM

In this section we construct an explicit model of MMGM. We take two sets of messengers, the first set consists of two pairs of SU(5) $5 + \bar{5}$ fields: $\phi_i, \bar{\phi}_i$ with $i = 1, 2$, and the second set contains a magic field: $\phi_3 = \phi_Q + \phi_{\bar{Q}} + \phi_G$. Note that one can write down the required terms for gauge mediation (as given in Eq. (9)) using only ϕ_3 and without invoking its conjugate field $\bar{\phi}_3$. Moreover, absence of the field $\bar{\phi}_3$ does not break the messenger parity because the superpotential remains invariant under the interchange of ϕ_Q by $\phi_{\bar{Q}}$ and vice versa. This is why we do not include the $\bar{\phi}_3$ field in the second set just to make it more economical. In the second set, we will denote the fermion mass by m_3 and the eigenvalues of the scalar mass squared matrix by $m_{\pm}^2 \pm d$. For the first set, in the diagonal basis of the fermion mass matrix $M_f = \text{diag}(m_1, m_2)$, the mass squared matrix of the scalars will look like,

$$M_{\pm}^2 = \begin{pmatrix} m_1^2 & 0 \\ 0 & m_2^2 \end{pmatrix} \pm \begin{pmatrix} a & b \\ b & c \end{pmatrix}. \quad (22)$$

Clearly the eigenvalues and the diagonalizing matrices of M_{\pm}^2 will involve the quantities a, b, c and hence, the four parameters $M_1, \tilde{\zeta}, A_1$ and η will also depend on them. Just to give few examples, in Table-I we choose six benchmark points ² and show the values of a, b, c, d and the corresponding numerical values for $M_1, \tilde{\zeta}, A_1$ and η .

Benchmark points	a	b	c	d	M_1 (GeV)	$\tilde{\zeta}$	A_1 (10^8 GeV ²)	η (10^{-5})
1	0.85	80	0.85	0.60	97.304	-0.1914	2.0534	-1.4061
2	0.80	70	0.80	0.90	95.165	-0.2794	1.5722	-4.1320
3	0.80	70	0.80	1.2	98.373	-0.3527	1.5722	-7.3458
4	0.80	70	0.80	1.4	100.51	-0.3989	1.5722	-9.9983
5	0.80	70	0.80	1.6	102.65	-0.4432	1.5723	-13.059
6	0.80	70	0.80	1.8	104.79	-0.4858	1.5723	-16.527

TABLE I. The values of a, b, c and d parameters for six benchmark points and the corresponding numerical values for the quantities $M_1, \tilde{\zeta}, A_1$ and η . The values of m_1, m_2 and m_3 are 1.0×10^{14} GeV. The parameters a, b, c and d are given in units of 10^{18} GeV².

It is well known that among the various models of GMSB, the mass ratio between the sfermions and gauginos is the lowest in case of ordinary gauge mediation models [20] (which can be obtained by setting $b = 0$ in Eq. (22)). In order to increase this ratio, b should be made large compared to a and c . The parameter d is related to the magic part of the model. So changing d , one can increase or decrease the splitting among the gaugino masses. Note that, we got $\tilde{\zeta} \sim 10^{-1}$ whereas $\eta \sim 10^{-5}$. So gaugino masses are highly hierarchical (see Table II) but A_a parameters are not. To understand this one should note that the SU(5) part of this model is not an OGM model but an EOGM model, and b is hundred times larger than a, c and d . From Eqn. (B.6) and (B.8) of [20], one can see that the off-diagonal element b has no effect on the expression for gaugino masses whereas it has dominant contribution on the sfermion masses. Using the fact that $\frac{F}{M^2} \sim 10^{-8}$, the expression for the η parameter can be approximated as: $\eta \sim -\frac{1}{4} \frac{d^2}{b^2}$. This explains why η is small in this model.

A. Phenomenology: boosted higgs signal

There are many models of supersymmetry breaking where the soft supersymmetry breaking gaugino mass terms M_1, M_2 and M_3 meet to a common value $m_{1/2}$ at the GUT scale. Now the one-loop Renormalization Group equations for the three gaugino mass parameters in the MSSM are determined by the same quantities b_a^0 ($a=1, 2, 3$) which also control the RG running of the three gauge couplings. It then immediately follows that each of the three ratios $\frac{M_a}{g_a^2}$ is one-loop RG invariant. In models of gaugino mass unification (for example, models with minimal supergravity or gauge-mediated boundary conditions) this leads to an interesting relation, $M_1:M_2:M_3 = 1:2:7$ approximately at the TeV scale (modulo two loop corrections and unknown threshold corrections). Now, if the supersymmetric Higgsino

² In our models, gravitino mass is in the range 17 GeV to 20 GeV. If we assume gravitino to be the LSP then Big Bang Neucleosynthesis will be problematic because of large neutralino lifetime. This problem can be easily solved in the axino dark matter models where life time of the lightest neutralino can be less than .1 sec[33–35].

mass parameter $\mu \gg M_1, M_2$ then the physical mass eigenstates consist of a ‘‘bino-like’’ lightest neutralino $\tilde{\chi}_1^0$ and a ‘‘wino-like’’ next-to-lightest neutralino $\tilde{\chi}_2^0$ and lightest chargino $\tilde{\chi}_1^\pm$. In this case one has to a very good approximation $m_{\tilde{g}} \sim M_3$, $m_{\tilde{\chi}_2^0}, m_{\tilde{\chi}_1^\pm} \sim M_2$ and $m_{\tilde{\chi}_1^0} \sim M_1$. With the increase of the lower bound on squark and gluino masses by the LHC data, their production cross section has been pushed to quite low values (\sim few fb). On the other hand the electro weak gauginos can be sufficiently lighter ($\tilde{\chi}_1^\pm, \tilde{\chi}_2^0 \sim 250$ is still allowed even if universality is assumed). Hence the pair production cross-section of the light electroweak gauginos dominate the SUSY production cross-section.

In our model, as we have already seen, in general the gaugino mass parameters can be arranged to have any ratio among themselves. In particular, we consider the case where M_1, M_2 and M_3 are much more hierarchical than the ratio 1:2:7. In this case $\tilde{\chi}_1^\pm$ and $\tilde{\chi}_2^0$ even lighter than 250 GeV are still allowed. In this section we consider the production of $\tilde{\chi}_1^\pm, \tilde{\chi}_2^0 \sim$ and their subsequent decays, $\tilde{\chi}_1^\pm \rightarrow \tilde{\chi}_1^0 W$ and $\tilde{\chi}_2^0 \rightarrow \tilde{\chi}_1^0 h$. The prospect of this channel at 8 TeV LHC in case of the mSUGRA model has been studied in detail in [37]. It was concluded that an integrated luminosity of 100 fb^{-1} will be needed for a good signal to background ratio. Note that, unlike mSUGRA in our model the lightest neutralino χ_1^0 can be considerably lighter than χ_2^0 and hence, the lightest Higgs boson from the decay of χ_2^0 can be quite boosted.

In Table-II we show a few benchmark points which will be used for a detail signal analysis. We choose the parameters in our model so as to get different ratios of gaugino masses along with the lightest Higgs boson mass consistent with the recent hints of Higgs signal by the CMS [39] and ATLAS [40] collaborations. Note that, in our case the branching ratio for the decay $\tilde{\chi}_2^0 \rightarrow \tilde{\chi}_1^0 h$ is very large ($> 95\%$). For related discussions on the parameter dependence on this branching ratio and interplay with other decay modes see the reference [41].

To generate the mass spectrum of the SUSY particles we have used the package SuSpect [42]. SUSYHIT [43] has been used to calculate the corresponding branching ratios. Note that the gluinos are quite heavy for all the benchmark points and consequently their production cross-section is extremely small. For example, for the benchmark point-1 the gluino pair production cross-section is about 4 fb (LO) for 8 TeV center of mass energy and it is even smaller for the other benchmark points.

Benchmark points	$\tan\beta$	$m_{\tilde{\chi}_1^\pm}$ (GeV)	$m_{\tilde{\chi}_2^0}$ (GeV)	$m_{\tilde{\chi}_1^0}$ (GeV)	m_h (GeV)	$m_{\tilde{g}}$ (GeV)	μ (GeV)	$\text{BR}(\chi_2^0 \rightarrow \chi_1^0 h)$	$\frac{\delta M_Z^2}{M_Z^2}(B\mu)$	$\frac{\delta M_Z^2}{M_Z^2}(\mu)$ (10^4)
1	20	203.0	203.0	50.9	124.8	1019	7935	98.908	66.25	1.53
2	25	248.1	248.1	49.0	124.6	1239	7003	96.883	30.83	1.19
3	30	299.4	299.4	50.2	124.8	1482	7024	95.221	19.74	1.19
4	20	332.3	332.3	50.6	124.8	1641	7055	96.076	52.64	1.21
5	20	366.1	366.1	51.3	124.9	1797	7070	95.621	52.92	1.21
6	20	399.7	399.7	51.9	124.9	1950	7085	96.343	53.19	1.22

TABLE II. Masses of the lightest neutralino, next-to-lightest neutralino, lightest chargino and lightest CP even neutral Higgs for the six benchmark points. All other SUSY particles have masses in the multi-TeV range (~ 7 TeV to 15 TeV). Definition of fine tuning parameters are $\frac{\delta M_Z^2}{M_Z^2}(\mu) = \frac{2\mu^2}{M_Z^2} \left[1 + t_\beta \frac{4 \tan^2 \beta (\tilde{m}_1^2 - \tilde{m}_2^2)}{(\tilde{m}_1^2 - \tilde{m}_2^2)t_\beta - M_Z^2} \right] \frac{\delta\mu^2}{\mu^2}$ and $\frac{\delta M_Z^2}{M_Z^2}(B\mu) = 4t_\beta \tan^2 \beta \frac{\tilde{m}_1^2 - \tilde{m}_2^2}{M_Z^2(\tan^2 \beta - 1)^2}$ where $t_\beta = (\tan^2 \beta + 1)/(\tan^2 \beta - 1)$. Hence fine-tuning is large.

In Fig.1 we show the transverse momentum distribution of the Higgs in the decay $\tilde{\chi}_2^0 \rightarrow \tilde{\chi}_1^0 h$ following the direct production of $\tilde{\chi}_1^\pm, \tilde{\chi}_2^0$ at the LHC with 8 TeV center of mass energy. It can be observed that a large fraction of the Higgs bosons has transverse momentum greater than 100 GeV. This allows us to use the jet substructure technique to look for Higgs in the decays of directly produced electroweak gauginos.

The use of jet substructure for the reconstruction of hadronic decays of boosted W, Z, Higgs bosons and top quarks has received considerable attention in recent years [45–47]. A study of jet substructure in the context of a search for a heavy Higgs boson decaying to W W was first carried out in Ref. [48]. More recently, Butterworth, Davison, Rubin and Salam(BDRS)[49] studied the case of a light Higgs boson ($m_H \sim 120$ GeV) produced in association with an electroweak gauge boson. The leptonic decay of the associated vector boson provides an efficient trigger for these events. The BDRS algorithm involves a technique using the mass-drop and the filtering to transform the high- p_T WH, ZH($H \rightarrow b \bar{b}$) channel into one of the best channels for discovery of Standard Model Higgs with small mass at the LHC.

In this section we adopt the BDRS method for tagging hadronically decaying Higgs boson. We describe below the exact procedure adopted in our analysis in order to implement this along with our other selection cuts.

We first cluster all the stable final state particles(excluding leptons, neutrinos and neutralinos) into ‘‘fat-jets’’ using the Cambridge-Aachen algorithm (CA algorithm) [50, 51] as implemented by the Fastjet package [52] with R parameter of 1.2. We then select the jets with transverse momentum $p_T > 100$ GeV and pseudo rapidity $|\eta| < 2.5$.

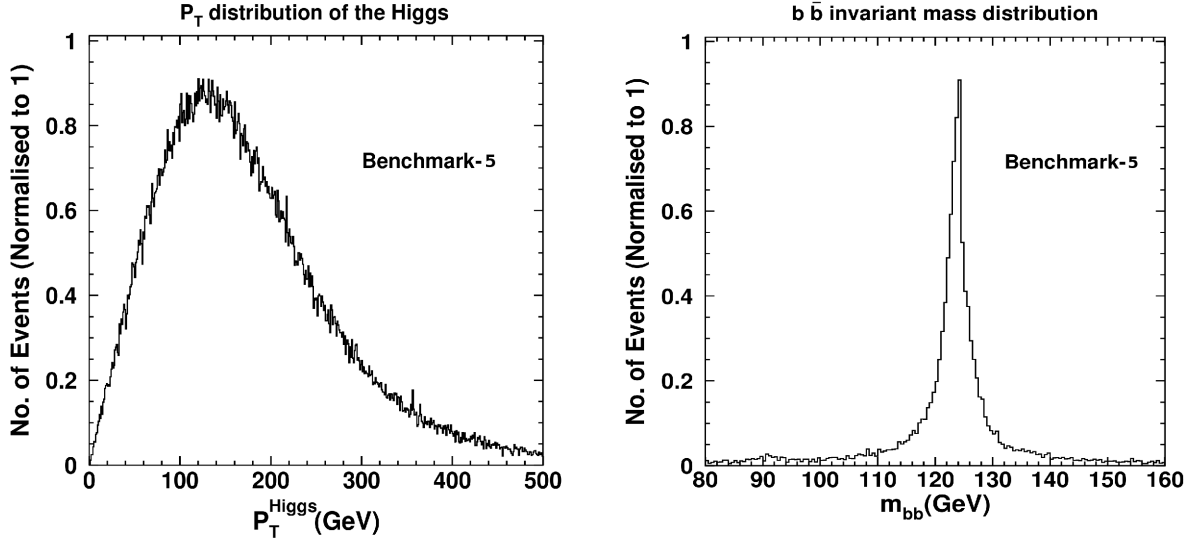


FIG. 1. Left panel : The transverse momentum distribution of the Higgs boson from the decay $\chi_2^0 \rightarrow \chi_1^0 h$ following the direct production of (χ_1^\pm, χ_2^0) at 8 TeV LHC for our SUSY benchmark point 5. The y-axis has been normalized to 1. Right panel: The invariant mass distribution of the reconstructed Higgs boson using the jet substructure algorithm, as described in the text, for our SUSY benchmark point 5. The y-axis has been normalized to 1. The figures have been generated using the CERN package PAW [44].

We now perform the jet substructure analysis on the hardest jet following the BDRS prescription. Here we closely follow the discussion of Ref. [49], mentioning our specific choices of parameters as and when the occasion arises. The first step is to select a jet- j and apply the following procedure:

1. Undo the last clustering step of the jet- j to get two subjets. Label the two subjets j_1 and j_2 so that $m_{j_1} > m_{j_2}$. (Remember that at each step during the CA clustering the masses of the proto-jets to be combined are recorded.)
2. Define $\mu = \frac{m_{j_1}}{m_j}$, $y_{\text{cut}} = \frac{\min(p_{T,j_1}^2, p_{T,j_2}^2)}{m_j^2} \Delta R_{j_1, j_2}^2$. Here $\Delta R_{j_1, j_2}$ is the separation between the two subjets j_1 and j_2 in the pseudo rapidity(η)- azimuthal angle(ϕ) plane. If $\mu < \mu_{\text{cut}}$ (significant mass drop) and $y > y_{\text{cut}}$ (the splitting of the hard jet- j into two subjets j_1 and j_2 is not too asymmetric) then go to step 4. We use $\mu_{\text{cut}} = 0.4$ and $y_{\text{cut}} = 0.1$ in our analysis.
3. Otherwise redefine $j = j_1$ and go back to step 1.
4. Take the constituents of the mother jet- j and recluster them with the Cambridge-Aachen algorithm with an R-parameter of $R_{\text{filt}} = \min(\frac{\Delta R_{j_1, j_2}}{2}, 0.4)$. Construct n new subjets $j_1^{\text{filt}}, j_2^{\text{filt}}, j_3^{\text{filt}}, \dots, j_n^{\text{filt}}$ ordered in descending p_T . This step is supposed to reduce the degradation of resolution on jets caused by underlying events.
5. Require the two hardest of the subjets $j_1^{\text{filt}}, \dots, j_n^{\text{filt}}$ to have b tags.
6. Define $j^{\text{higgs}} = \sum_{i=1}^{\min(n,3)} j_i^{\text{filt}}$. This step captures the dominant $\mathcal{O}(\alpha_s)$ radiation from the Higgs decay, while eliminating much of the contamination from underlying events[49].

The parameters involved in this method can be, in principle, optimized event by event [53]. In our analysis, these parameters have been set to fixed values as already mentioned above. In Fig. 1 we show the distribution of the reconstructed Higgs mass using the above BDRS prescription for our SUSY benchmark point-5. For the other benchmark points the distributions are qualitatively same and we do not show them here.

We also impose a b-jet reconstruction efficiency of 70% [54] in our analysis. We then require the following pre-selection cuts [36–38]:

Process	Crosssection (LO)	Simulated Events	Number of Events after individual cuts					Crosssection after Cut-V	$\frac{S}{\sqrt{B}}$ (30 fb ⁻¹)
			Cut-I	Cut-II	Cut-III	Cut-IV	Cut-V		
Signal									
Benchmark-1	533 fb	50K	681	178	71	47	28	0.21 fb	≈ 4
Benchmark-2	241 fb	50K	1220	311	150	106	84	0.27 fb	≈ 5.1
Benchmark-3	108 fb	50K	1729	475	287	201	177	0.27 fb	≈ 5.1
Benchmark-4	71 fb	50K	2112	552	356	270	246	0.23 fb	≈ 4.4
Benchmark-5	45 fb	50K	2697	788	522	380	341	0.21 fb	≈ 4
Benchmark-6	30 fb	50K	3092	904	655	488	449	0.21 fb	≈ 4
Background									
t t(0-100)	48.3 pb	40L	1126	274	29	3	0		
t t(100-200)	36.6 pb	30L	976	234	26	6	1	0.0119 fb	
t t(200-300)	7.8 pb	5L	157	40	6	3	2	0.0306 fb	
t t(300-500)	1.8 pb	1.5L	24	5	1	0	0		
t t(500-∞)	134 fb	10K	0	0	0	0	0		
W(→ lν _l) b b l = e, μ, τ	3 pb	201308	64	35	3	2	0		
W h	549 fb	50K	401	125	9	5	2	0.0108	
W Z	13 pb	8L	11	3	0	0	0		
Z h	296 fb	20K	167	4	0	0	0		
Z(→ l ⁺ l ⁻)bb l = e, μ, τ	2 pb	126581	26	5	0	0	0		
t(→ eν _e) b b	308 fb	36817	6	5	0	0	0		
t b W	18.7 pb	597812	156	43	4	2	2	0.0306 fb	
Total Background								0.084 fb	

TABLE III. Event summary for the signal and the backgrounds after individual cuts as described in the text for LHC8. In the second column, the Leading Order (LO) cross-sections have been obtained using PYTHIA and ALPGEN. While calculating the final crosssection after Cut-V, the NLO cross-sections for signal(from PROSPINO) and appropriate K factors (whenever available) for the backgrounds, as mentioned in the text, have been used. The b-tagging efficiency has also been multiplied. K and L in the third column stand for 10³ and 10⁵ respectively. Note that the number of simulated events is always more than the expected number of events at LHC (at 30 fb⁻¹) for both the signal and backgrounds.

- Cut-I : We require the mass of j^{higgs} to be in the window [119, 129].
- Cut-II : Exactly one isolated lepton(ℓ) with $p_T(\ell) > 20\text{GeV}$ and no isolated lepton with $10\text{ GeV} < p_T(\ell) < 20\text{ GeV}$.
- Cut-III : The transverse mass of the lepton(ℓ)-missing P_T system $M_T^{(\ell P_T)} > 90\text{ GeV}$.
- Cut-IV : At this stage we again construct “normal“ jets using the CA algorithm with R parameter of 0.5, $|\eta| < 2.5$, $P_T > 50\text{ GeV}$. We then calculate H_T , which is defined as the scalar sum of the P_T 's of all these ”normal“ jets. We define $R_T^{b\bar{b}} = \frac{p_{Tb_1} + p_{Tb_2}}{H_T}$. Remember that p_{Tb_1} and p_{Tb_2} are the transverse momenta of the two subjects j_1^{flit} and j_2^{flit} which are by now identified as two b-jets. We demand $R_T^{b\bar{b}} > 0.9$.
- Cut-V : Events are selected with $P_T > 125\text{ GeV}$.

In Table-III and Table-IV we show the signal and backgrounds after each selection cut for 8TeV and 14TeV center of mass energies respectively. For all the signal points we use the NLO cross-section from Prospino[55]. We simulate the $t\bar{t}$, Wh, WZ and Zh backgrounds using PYTHIA[56]. For the Wbb, Zbb and single top backgrounds we generate the unweighted event files in ALPGEN [57] and then use the ALPGEN-PYTHIA interface (including matching of the matrix element hard partons and shower generated jets, following the MLM prescription[58]) to perform the showering and implement our event selection cuts. For the tt background a K factor of 2 has been used. We use the CTEQ6L parton distribution functions and set top mass at 172.9 GeV in our analysis. We have also used the new LHC PYTHIA 6.4 Tune Z2* for the correct description of the Underlying events[59]. We see that a S/\sqrt{B} about 4-6 can be obtained at 8TeV LHC with an integrated luminosity of about 30 fb⁻¹. At the 14TeV LHC the situation is much better and even with 15 fb⁻¹ we get fairly good number of events, while the backgrounds are totally under control with our selection cuts. In Table-III (Table-IV) we have simulated at least 30 fb⁻¹ (15 fb⁻¹) of events for

Process	Crosssection (LO)	Simulated Events	Number of Events after individual cuts					Crosssection after Cut-V
			Cut-I	Cut-II	Cut-III	Cut-IV	Cut-V	
Signal								
Benchmark-1	1.4 pb	50K	769	186	78	54	29	0.53 fb
Benchmark-2	681 fb	50K	1282	327	156	119	92	0.73 fb
Benchmark-3	332 fb	50K	1857	465	288	198	169	0.73 fb
Benchmark-4	226 fb	50K	2363	626	392	274	238	0.73 fb
Benchmark-5	155 fb	50K	2792	746	499	359	321	0.67 fb
Benchmark-6	105 fb	50K	3125	843	592	416	373	0.53 fb
Background								
t t(50-∞)	335 pb	100L	3467	913	128	11	3	0.098 fb
W(→ l ν _l) b b l = e, μ, τ	5.45 pb	429871	148	86	7	6	0	
W h	1.24 pb	50K	446	108	7	3	1	0.012 fb
W Z	29 pb	8L	20	5	0	0		
Z h	674 fb	50K	449	6	0	0	0	
Z(→ ℓ ⁺ ℓ ⁻)bb ℓ = e, μ, τ	7.4 pb	607607	116	23	5	4	0	
t b	5.6 pb	182974	16	3	0	0	0	
t(→ ℓ ν _ℓ) b b W (→ had) ℓ = e, μ, τ	17.1 pb	499383	125	65	11	0	0	
t(→ had) b W (→ ℓ ν _ℓ) ℓ = e, μ, τ	17.1 pb	665454	229	127	14	3	0	
Total Background								0.11 fb

TABLE IV. Event summary for the signal and the backgrounds after individual cuts as described in the text for LHC14. In the second column, the Leading Order (LO) cross-sections have been obtained using PYTHIA and ALPGEN. While calculating the final crosssection after Cut-V, the NLO cross-sections for signal(from PROSPINO) and appropriate K factors (whenever available) for the backgrounds, as mentioned in the text, have been used. The b-tagging efficiency has also been multiplied. K and L in the third column stand for 10^3 and 10^5 respectively. Note that the number of simulated events is always more than the expected number of events at LHC (at 15 fb^{-1}) for both the signal and backgrounds.

both the signal points as well as the backgrounds. Note that detector and other experimental effects will degrade the signal significance somewhat. We have checked that the numbers change by $\sim 10\%$ if a Gaussian smearing is added to the transverse momenta of the jets and the missing transverse momentum, though a faithful quantification of the detector effects is beyond the scope of this work.

As the masses of $\tilde{\chi}_1^\pm$ and $\tilde{\chi}_2^0$ increase (see Table.II), their production cross-section gradually decreases. This tends to reduce the signal to background ratio. But on the other hand from the benchmark-1 to benchmark-6 the mass difference between $\tilde{\chi}_2^0$ and $\tilde{\chi}_1^0$ also increases. This makes the Higgs boson more boosted thereby increasing the efficiency of the jet substructure algorithm. With the increasing mass of $\tilde{\chi}_2^0$ in Table.II these two opposite effects keep competing with each other. This is why the signal efficiency initially increases with increasing $\tilde{\chi}_2^0$ mass but again starts falling down because of the rapid decrease in the crosssection.

V. CONCLUSION

In this paper we have implemented magic fields as messengers of SUSY breaking in GMSB. One of the advantages of using magic fields as messengers over other generalized messengers is that achievement of unification is independent of the masses of the magic messengers.

In our model the gaugino sector is parameterized by only two independent parameters, one of them can be taken to be the U(1) gaugino mass and the second one being the ζ parameter (Eq. (14) and (15)). The ζ parameter can be tuned to get various hierarchies among the gaugino masses which can lead to distinct phenomenological consequences.

The sfermion sector can also be characterized by only two independent quantities. These are the U(1) A-parameter A_1 (Eq. 18) and the parameter η (Eq. 21). Choosing η , different hierarchies between the squark and slepton masses can be achieved. When the value of η is close to its upper limit η_0 , the squark and Higgs masses at the messenger scale

tend to be almost same. This allows one to have small μ parameter and Higgsino-like NLSP similar to the models of EOGM with large doublet-triple splitting.

We focus on the region of parameter space where a comparatively larger splitting (about 1:6) between the U(1) and SU(2) gaugino masses is achieved along with the lightest supersymmetric Higgs boson mass about 125 GeV. We consider the direct electroweak production of χ_1^\pm and χ_2^0 with χ_1^\pm decaying to the lightest neutralino χ_1^0 and a W boson, and χ_2^0 decaying to χ_1^0 and the lightest Higgs h . Because of the large splitting between χ_2^0 and χ_1^0 , the produced Higgs boson is expected to have quite large transverse momentum. Motivated by this we have analyzed the $\ell + b \bar{b} + \cancel{E}_T$ channel using the jet substructure technique. We have simulated all possible backgrounds for this final state and conclude that while $S/\sqrt{B} \sim 4 - 6$ is viable (for the mass ranges of charginos and neutralinos we have considered) at 8 TeV LHC with a integrated luminosity of 30 fb^{-1} , LHC14 can do much better and even with 15 fb^{-1} of data a decent number of signal events over the backgrounds is expected. In our analysis, we have not considered any detector effect which is expected to degrade the signal significance to some extent.

A detailed exploration of other phenomenological consequences of this class of models including constraints from Flavor physics as well as other low energy experiments should be carried out and we plan to perform such a study in a future publication [60].

VI. ACKNOWLEDGEMENT

PB would like to thank Prof. Palash B. Pal for encouragement and Diego Marques for some comments. PB is also grateful to Prof. Amol Dighe for his kind hospitality at the Department of Theoretical Physics of TIFR where a large part of this project was completed. DG thanks Prof. Monoranjan Guchait and Dr. Dipan Sengupta for insightful discussions and technical help in the event simulation. DG would also like to thank Prof. Amol Dighe for his continuous support.

-
- [1] Sandra Kortner, ATLAS Collaboration, presentation at *the XLVIIIth Rencontres de Moriond, Electroweak session*, March 7, 2012, ATLAS-CONF-2012-019.
 - [2] Marco Pieri, CMS Collaboration, presentation at *the XLVIIIth Rencontres de Moriond, Electroweak session*, March 7, 2012.
 - [3] Steven Lowette, on behalf of the ATLAS and CMS collaborations, presentation at *the XLVIIIth Rencontres de Moriond, Electroweak session*, March 8, 2012.
 - [4] J. Wess and J. Bagger, “Supersymmetry and supergravity,” *Princeton, USA: Univ. Pr. (1992)*.
 - [5] S. P. Martin, “A Supersymmetry primer,” In *Kane, G.L. (ed.): Perspectives on supersymmetry II* 1-153 [hep-ph/9709356].
 - [6] H. P. Nilles, Phys. Rept. **110**, 1 (1984).
 - [7] M. Dine, W. Fischler and M. Srednicki, Nucl. Phys. B **189** (1981) 575.
 - [8] S. Dimopoulos and S. Raby, Nucl. Phys. B **192** (1981) 353.
 - [9] M. Dine and W. Fischler, Phys. Lett. B **110** (1982) 227.
 - [10] M. Dine and W. Fischler, Nucl. Phys. B **204** (1982) 346.
 - [11] G. F. Giudice and R. Rattazzi, Phys. Rept. **322**, 419 (1999) [hep-ph/9801271].
 - [12] C. R. Nappi and B. A. Ovrut, Phys. Lett. B **113** (1982) 175.
 - [13] P. Meade, N. Seiberg and D. Shih, Prog. Theor. Phys. Suppl. **177**, 143 (2009) [arXiv:0801.3278 [hep-ph]].
 - [14] J. Distler and D. Robbins, arXiv:0807.2006 [hep-ph].
 - [15] K. A. Intriligator and M. Sudano, JHEP **0811**, 008 (2008) [arXiv:0807.3942 [hep-ph]].
 - [16] Z. Komargodski and N. Seiberg, JHEP **0903**, 072 (2009) [arXiv:0812.3900 [hep-ph]].
 - [17] L. M. Carpenter, M. Dine, G. Festuccia and J. D. Mason, arXiv:0805.2944 [hep-ph].
 - [18] M. Buican, P. Meade, N. Seiberg and D. Shih, arXiv:0812.3668 [hep-ph].
 - [19] T. Kobayashi, Y. Nakai and R. Takahashi, JHEP **1001**, 003 (2010) [arXiv:0910.3477 [hep-ph]].
 - [20] T. T. Dumitrescu, Z. Komargodski, N. Seiberg and D. Shih, JHEP **1005**, 096 (2010) [arXiv:1003.2661 [hep-ph]].
 - [21] S. P. Martin, Phys. Rev. D **55**, 3177 (1997) [hep-ph/9608224].
 - [22] D. Marques, JHEP **0903**, 038 (2009) [arXiv:0901.1326 [hep-ph]].
 - [23] L. Calibbi, L. Ferretti, A. Romanino and R. Ziegler, Phys. Lett. B **672**, 152 (2009) [arXiv:0812.0342 [hep-ph]].
 - [24] C. Cheung, A. L. Fitzpatrick and D. Shih, JHEP **0807**, 054 (2008) [arXiv:0710.3585 [hep-ph]].
 - [25] S. P. Martin and P. Ramond, Phys. Rev. D **51**, 6515 (1995) [hep-ph/9501244].
 - [26] H. Kawase, N. Maekawa and K. Sakurai, JHEP **1001**, 027 (2010) [arXiv:0910.5555 [hep-ph]].
 - [27] J. L. Feng, K. T. Matchev and T. Moroi, Phys. Rev. Lett. **84**, 2322 (2000) [hep-ph/9908309].
 - [28] J. L. Feng, K. T. Matchev and T. Moroi, Phys. Rev. D **61**, 075005 (2000) [hep-ph/9909334].
 - [29] K. Agashe and M. Graesser, Nucl. Phys. B **507**, 3 (1997) [hep-ph/9704206].
 - [30] K. Agashe, Phys. Rev. D **61**, 115006 (2000) [hep-ph/9910497].

- [31] J. T. Ruderman and D. Shih, arXiv:1103.6083 [hep-ph].
- [32] Y. Kats, P. Meade, M. Reece and D. Shih, JHEP **1202**, 115 (2012) [arXiv:1110.6444 [hep-ph]].
- [33] T. Asaka and T. Yanagida, Phys. Lett. B **494**, 297 (2000) [hep-ph/0006211].
- [34] L. Covi, J. E. Kim and L. Roszkowski, Phys. Rev. Lett. **82** (1999) 4180 [hep-ph/9905212].
- [35] L. Covi, H. -B. Kim, J. E. Kim and L. Roszkowski, JHEP **0105** (2001) 033 [hep-ph/0101009].
- [36] M. Guchait and D. Sengupta, Phys. Rev. D **84**, 055010 (2011) [arXiv:1102.4785 [hep-ph]].
- [37] D. Ghosh, M. Guchait and D. Sengupta, arXiv:1202.4937 [hep-ph].
- [38] D. Ghosh, M. Guchait, S. Raychaudhuri and D. Sengupta, arXiv:1205.2283 [hep-ph].
- [39] S. Chatrchyan *et al.* [CMS Collaboration], “Combined results of searches for the standard model Higgs boson in pp collisions at $\sqrt{s} = 7$ TeV,” arXiv:1202.1488 [hep-ex].
- [40] [ATLAS Collaboration], “Combined search for the Standard Model Higgs boson using up to 4.9 fb^{-1} of pp collision data at $\sqrt{s} = 7$ TeV with the ATLAS detector at the LHC,” arXiv:1202.1408 [hep-ex].
- [41] S. Gori, P. Schwaller and C. E. M. Wagner, Phys. Rev. D **83**, 115022 (2011) [arXiv:1103.4138 [hep-ph]].
- [42] A. Djouadi, J. -L. Kneur and G. Moultaka, Comput. Phys. Commun. **176**, 426 (2007) [hep-ph/0211331].
- [43] A. Djouadi, M. M. Muhlleitner and M. Spira, Acta Phys. Polon. B **38**, 635 (2007) [hep-ph/0609292].
- [44] Physics Analysis Workstation (PAW), <http://wwwasd.web.cern.ch/wwwasd/paw/>
- [45] G. D. Kribs, A. Martin, T. S. Roy and M. Spannowsky, Phys. Rev. D **82**, 095012 (2010) [arXiv:1006.1656 [hep-ph]].
- [46] A. Abdesselam, E. B. Kuutmann, U. Bitenc, G. Brooijmans, J. Butterworth, P. Bruckman de Renstrom, D. Buarque Franzosi and R. Buckingham *et al.*, Eur. Phys. J. C **71**, 1661 (2011) [arXiv:1012.5412 [hep-ph]].
- [47] A. Altheimer, S. Arora, L. Asquith, G. Brooijmans, J. Butterworth, M. Campanelli, B. Chappleau and A. E. Cholakian *et al.*, arXiv:1201.0008 [hep-ph].
- [48] M. H. Seymour, Z. Phys. C **62**, 127 (1994).
- [49] J. M. Butterworth, A. R. Davison, M. Rubin and G. P. Salam, Phys. Rev. Lett. **100**, 242001 (2008) [arXiv:0802.2470 [hep-ph]].
- [50] Y. L. Dokshitzer, G. D. Leder, S. Moretti and B. R. Webber, JHEP **9708**, 001 (1997) [hep-ph/9707323].
- [51] M. Wobisch and T. Wengler, In *Hamburg 1998/1999, Monte Carlo generators for HERA physics* 270-279 [hep-ph/9907280].
- [52] M. Cacciari and G. P. Salam, Phys. Lett. B **641**, 57 (2006) [hep-ph/0512210].
- [53] D. E. Kaplan, K. Rehermann, M. D. Schwartz and B. Tweedie, Phys. Rev. Lett. **101**, 142001 (2008) [arXiv:0806.0848 [hep-ph]].
- [54] CMS collaboration Report NO.CMS-PAS-BTV-11-001.
- [55] W. Beenakker, R. Hopker and M. Spira, hep-ph/9611232.
- [56] T. Sjostrand, S. Mrenna and P. Z. Skands, JHEP **0605**, 026 (2006) [hep-ph/0603175].
- [57] M. L. Mangano, M. Moretti, F. Piccinini, R. Pittau and A. D. Polosa, JHEP **0307**, 001 (2003) [hep-ph/0206293].
- [58] J. Alwall, S. Hoche, F. Krauss, N. Lavesson, L. Lonnblad, F. Maltoni, M. L. Mangano and M. Moretti *et al.*, Eur. Phys. J. C **53**, 473 (2008) [arXiv:0706.2569 [hep-ph]].
- [59] Talk by A. Knutsson at CERN”, <http://indico.cern.ch/getFile.py/access?contribId=13&sessionId=2&resId=0&materialId=slides&confId=140054>
- [60] Pritibhajan Byakti, Diptimoy Ghosh – In preparation.